Published in : Solid State Sciences (2010), vol. 12, pp. 1490-1495.
Status : Postprint (Author's version)

Enhancement of the power factor of $[Bi_{1.68}Ca_2O_4]^{RS}[CoO_2]_{1.69}$ Ag composites prepared by the spray-drying method

B. Rivas-Murias[a], H. Muguerra[a], M. Traianidis[b], C. Henrist[a], B. Vertruyen[a], R. Cloots[a]

[a] *SUPRATECS/Inorganic Materials Chemistry, Department of Chemistry, University of Liège, Allée de la Chimie 3 (Bât. B6a), 4000 Liège, Belgium*

[b] *Belgian Ceramic Research Centre, Avenue Gouverneur Cornez 4, 7000 Mons, Belgium*

ABSTRACT

$[Bi_{1.68}Ca_2O_4]^{RS}[CoO_2]_{1.69}$ (BCCO) sample and Ag-BCCO composites (with 10, 20 or 30 wt% Ag) have been prepared by the spray-drying technique and uniaxially/isostatically packed. Scanning electron microscopy reveals that the Ag particles are well distributed in the BCCO cobaltite matrix at low Ag contents. The Ag particles have an important effect on densification and grain orientation of the samples, with a direct impact on their electrical conductivity. The electrical conductivity is higher for the uniaxial samples and increases with the Ag content up to 20% in weight, while the Seebeck coefficient is hardly affected. These features induce an improvement of the power factor, reaching a maximum value of 2.2 μW K^{-2} cm^{-1} at ~ 1050 K for the uniaxial sample with 20 wt% Ag. Our results suggest that the spray-drying technique is a promising method to obtain composites with a well-dispersed secondary phase.

Keywords : Oxides ; Layered cobaltite ; Composite ; Spray-drying technique ; Thermoelectric properties

1. Introduction

Thermoelectric (TE) devices have attracted an increasing attention due to their promising energy-conversion properties, combined with a small environmental impact. Converting even a small fraction of the waste heat released by automobiles or factories into electricity could lead to a large saving in energy consumption. The TE performance is evaluated by the dimension-less figure of merit $ZT = S^2\sigma T/\kappa$, where S, σ and κ are the Seebeck coefficient, the electrical conductivity and the thermal conductivity, respectively. Consequently, high S, high σ and low κ are required to improve the TE efficiency. Nevertheless, obtaining materials with such properties is not easily realizable as these three parameters are interrelated to each other; in general a σ increase leads to an S decrease and a κ increase.

The most effective thermoelectric modules ($ZT > 1$) are composed of intermetallic compounds, such as Bi_2Te_3 or PbTe [1-3], Two approaches are usually investigated to enhance the thermoelectric performances in such materials. One is minimizing the thermal conductivity by promoting phonon scattering and localization [4,5], The other is through the quantum confinement effect in reduced dimensionalities [6,7]. In addition, the search for new materials and new concepts is still very active, for example interesting properties recently reported for silver chalcogenide halides [8] or In_4Se_{3-d} [9].

However, the practical application of these materials is frequently hindered by some problems, such as their low melting or decomposition temperatures, their content of harmful or scarce elements and their high cost. Recently, layered cobalt oxides have attracted attention as promising thermoelectric materials because of their potential to overcome the above-mentioned problems and exhibit reasonably good thermoelectric performance at high temperatures in oxidizing atmosphere [10-14], The general chemical formula for these cobaltites may be given by $[M_mA_2O_{2+m}]^{RS}[CoO_2]_q$, where M = Bi,Pb,Co..., A = Ca,Sr,Ba... and $q = b_1/b_2$ is the incommensurate ratio. Their structure is formed by two monoclinic subsystems alternating along the c-axis: a CoO_2 layer (CdI_2-type), formed by CoO_6 edge sharing octahedra and a Rock-Salt-type (RS) block. The two subsystems share the same a and c crystallographic parameters but present different b parameters (b_1 and b_2 for RS block and CoO_2 layer, respectively).

The *ZT* figure of merit of these layered oxides is however rather low, well below *ZT* = 1 except for single crystals which are unpractical for applications. Optimization of the electrical properties in the polycrystalline layered compounds can be achieved by different ways: the texturation of polycrystalline materials [15-19], the modification of their crystallographic framework by ionic substitutions [20-23], and the synthesis of composites by addition of a material with a lower electrical resistivity [24-27].

Based on this last concept, the present work describes the influence of Ag addition on the properties of the promising thermoelectric material $[Bi_{1.68}Ca_2O_4]^{RS}[CoO_2]_{1.69}$ (BCCO) [18,23,28]. As reported in the literature for $Ca_3Co_4O_9$ [26,29-31] and $Na_xCoO_{2-\delta}$ [24,25,32], Ag addition is expected to be beneficial for the electrical conductivity, due to a better connection between the cobaltite grains. Moreover, we have studied how the microstructure of the composite of BCCO platelets and isotropic Ag particles is influenced by the type of packing (uniaxial or isostatic).

The spray-drying technique [33] is employed here to synthesize the Ag-cobaltite composites in one step. Aqueous precursor syntheses are an efficient way to obtain a good dispersion of the Ag particles in the cobaltite matrix in comparison with the classic solid state mixing method [25,30,32,34]. In this paper, we show that spray-drying is a successful alternative synthesis to get homogeneous systems.

2. Experimental

$[Bi_{1.68}Ca_2O_4]^{RS}[CoO_2]_{1.69}$ (BCCO) and Ag-BCCO composites containing 10, 20 and 30 wt% Ag were synthesized by heat treatment of precursor powders obtained by the spray-drying technique. For each composition, stoichiometric amounts of $CaCO_3$, $Co(CH_3COO)_2{\cdot}4H_2O$, $Bi(CH_3COO)_3$ and $AgNO_3$, as Ag source, were dissolved in aqueous acetic acid. The final cation concentration was ~0.1 mol/L and the solution pH was ~5. The solutions were sprayed at 1.4 mL/min in a co-current Büchi Mini Spray Dryer B191, using a 0.7 mm nozzle and a 700 normal L/h air flow. The inlet and outlet temperatures were 472 K and 418-423 K, respectively. The as-sprayed precursors were slowly heated (25 K/h) in air at 873 K for 2 h. To compare the thermoelectric properties, a BCCO sample was also synthesized by solid state reaction (1123 K, 10 h) from stoichiometric amounts of $CaCO_3$, Co_3O_4 and Bi_2O_3. For all compositions, two series of pellets were prepared: (i) by uniaxial pressing (P ~ 100 MPa) and (ii) by isostatic pressing (P ~ 225 MPa). Then, the pellets were sintered in air at 1123 K for 10 h in alumina crucibles. Finally, bar-shaped samples (2-3 × 1.5 × 14 mm^3) were cut and polished for transport property measurements.

X-ray powder diffraction (XRD) was performed using a Siemens D5000 diffractometer at room temperature with Cu (Kα) radiation, in the 2θ range from 10° to 70° with a step width of 0.020°. The patterns were analyzed by the Rietveld method using the JANA2000 program [35]. The microstructure was studied by scanning electron microscopy (Philips XL30 FEG-ESEM) and the cationic composition was determined by Energy Dispersive X-ray analysis (EDAX system). The density of the samples was measured by Archimedes' method in 1-butanol, using theoretical X-ray density values of 6.35 g/cm^3 for BCCO and 10.49 g/cm^3 for metallic silver [36]. The Seebeck coefficient and the electrical conductivity were simultaneously measured in air from 300 to 1100 K using a commercial RZ2001i device (Ozawa Science).

3. Results and discussion

3.1. Structural and microstructural characterization

Fig. 1 shows the X-Ray Diffraction (XRD) patterns of the $[Bi_{1.68}Ca_2O_4]^{RS}[CoO_2]_{1.69}$ (BCCO) sample and the Ag-$[Bi_{1.68}Ca_2O_4]^{RS}[CoO_2]_{1.69}$ (Ag-BCCO) composites obtained by spray-drying. The pattern of the BCCO sample corresponds to a single phase. For the Ag-BCCO composites, all diffraction peaks are identified as BCCO and metallic silver cubic phase [23,36], no impurities (such as Co_3O_4, often present in solid state samples) are detected. The intensity of the peaks of the Ag phase increases with the nominal Ag content (inset of Fig. 1). The results of the full pattern matching analysis are shown in Table 1. The cell parameters of the BCCO phase are not significantly modified in the Ag-BCCO composites and agree with those reported by Muguerra et al. [37] for a single crystal, a = 4.90 Å, b_1 = 4.71 Å, b_2 = 2.79 Å, c = 14.67 Å and β = 93.32° (b_1 for the RS block and b_2 for the CoO_2 layer). In addition, the different cation ratios obtained by Energy Dispersive X-ray analysis agree with the nominal composition of the single crystal BCCO phase [37], within experimental error (Table 1). This suggests that the majority of Ag is present in metallic form at the grain boundaries of BCCO and does not enter significantly into the crystal lattice. Indeed Ag substitution in the Ca or Bi crystallographic sites would lead to a modification of the cell parameters due to the difference of ionic radii (1.15 Å for Ag^+, 1.00 Å for Ca^{2+} and 1.03 Å for Bi^{3+} [38]). For example, Wang et al. [29] have reported a decrease of a and b_1 parameters and an increase

Published in : Solid State Sciences (2010), vol. 12, pp. 1490-1495.
Status : Postprint (Author's version)

of *c* parameter in the case of Ag substitution in $Ca_{3-x}Ag_xCo_4O_{9+\delta}$ cobaltite (x = 0.05-0.3). In conclusion, the behavior of the BCCO samples seems closer to the $Na_xCoO_{2-\delta}$ family, where metallic Ag secondary phases are observed for rather low nominal Ag substitution [32,39]. Similarly, our attempts to prepare a substituted BCCO sample yielded polyphasic materials.

Fig. 1. *X-ray diffraction patterns of the sintered samples (a) without Ag, (b) with 10 wt% Ag, (c) with 20 wt% Ag and (d) with 30 wt% Ag. The reflections of the metallic Ag cubic phase are marked by ● symbols.*

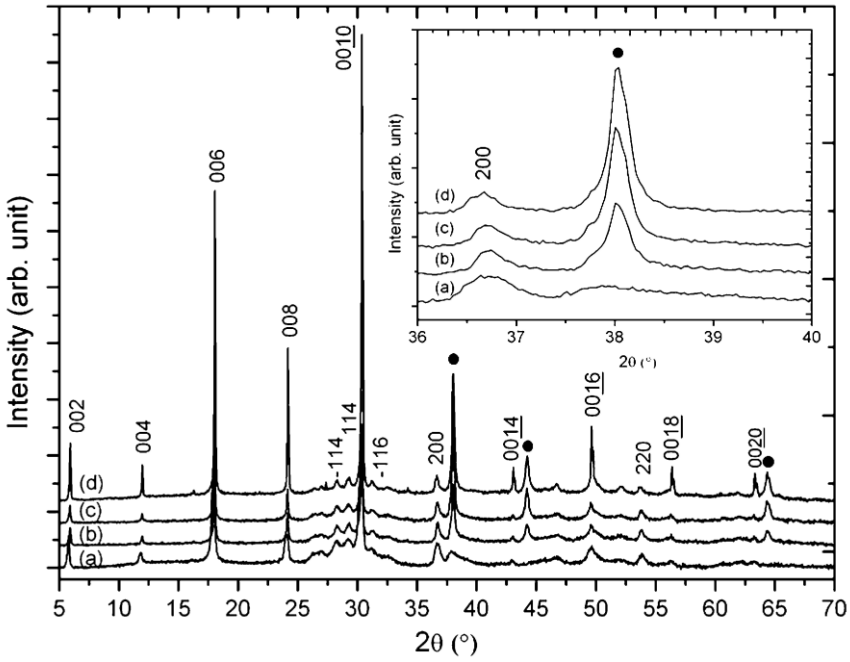

Table 1 *Cation ratios, crystallographic parameters and percentage of theoretical density (theoretical X-ray density values of 6.35 g/cm^3 for BCCO and 10.49 g/cm^3 for metallic silver) of the BCCO phase in the single phase and Ag-BCCO composite samples.*

Sample	Analyzed Composition Bi:Ca:Co	a (Å)	b_1 (Å)	b_2 (Å)	c (Å)	β (°)	Density (%)		$q = b_1/b_2$
							Uni	Iso	
BCCO single crystal [37]	1.68:2:1.69	4.9069(4)	4.7135(7)	2.7878(9)	14.668(5)	93.32(1)	-	-	1.6907(2)
BCCO spray-drying	1.65:1.98:1.69	4.90(9)	4.71(6)	2.78(9)	14.64(3)	93.3(2)	75	65	1.69(1)
BCCO 10wt% Ag	1.60:1.94:1.69	4.90(6)	4.72(7)	2.79(3)	14.68(5)	93.2(6)	65	61	1.69(2)
BCCO 20wt% Ag	1.62:1.96:1.69	4.90(4)	4.72(6)	2.79(5)	14.67(3)	93.2(7)	60	65	1.69(1)
BCCO 30wt% Ag	1.66:1.96:1.69	4.90(5)	4.72(3)	2.79(2)	14.67(4)	93.3(6)	72	61	1.69(2)

The microstructure of the as-sprayed particles displays a typical spherical shape, which transforms into platelets after treatment at 1123 K (with typical size below 5 µm in the ab plane, Fig. 2a), due to the layered structure of bismuth cobaltite. Fig. 2b-d presents backscattering electron micrographs of polished cross-sections of the Ag-BCCO composite samples. Metallic Ag particles appear as light gray zones in the darker BCCO matrix. In the case of the sample with 10 wt% Ag (Fig. 2b), the Ag particles are small (spherical shape inferior to 2 µm) and present a narrow size distribution (between 0.2 and 2 µm). For 20 wt% Ag (Fig. 2c), coexistence between small (~0.2 µm) and larger (~4 µm) particles is observed. Finally for 30 wt% Ag (Fig. 2d), the smallest Ag particles are ~2 µm and most Ag particles form large agglomerates (~12 µm). The electron micrographs of cross-sections of the uni-axially and isostatically-pressed BCCO samples (Fig. 3) show a more parallel stacking in the uniaxial sample.

Fig. 2. *(a) Secondary electron micrograph of the powder of BCCO sample; back scattered electron micrographs of polished cross-sections of composites containing (b) 10 wt% Ag, (c) 20 wt% Ag and (d) 30 wt% Ag. Ag particles are the light gray spots (circles).*

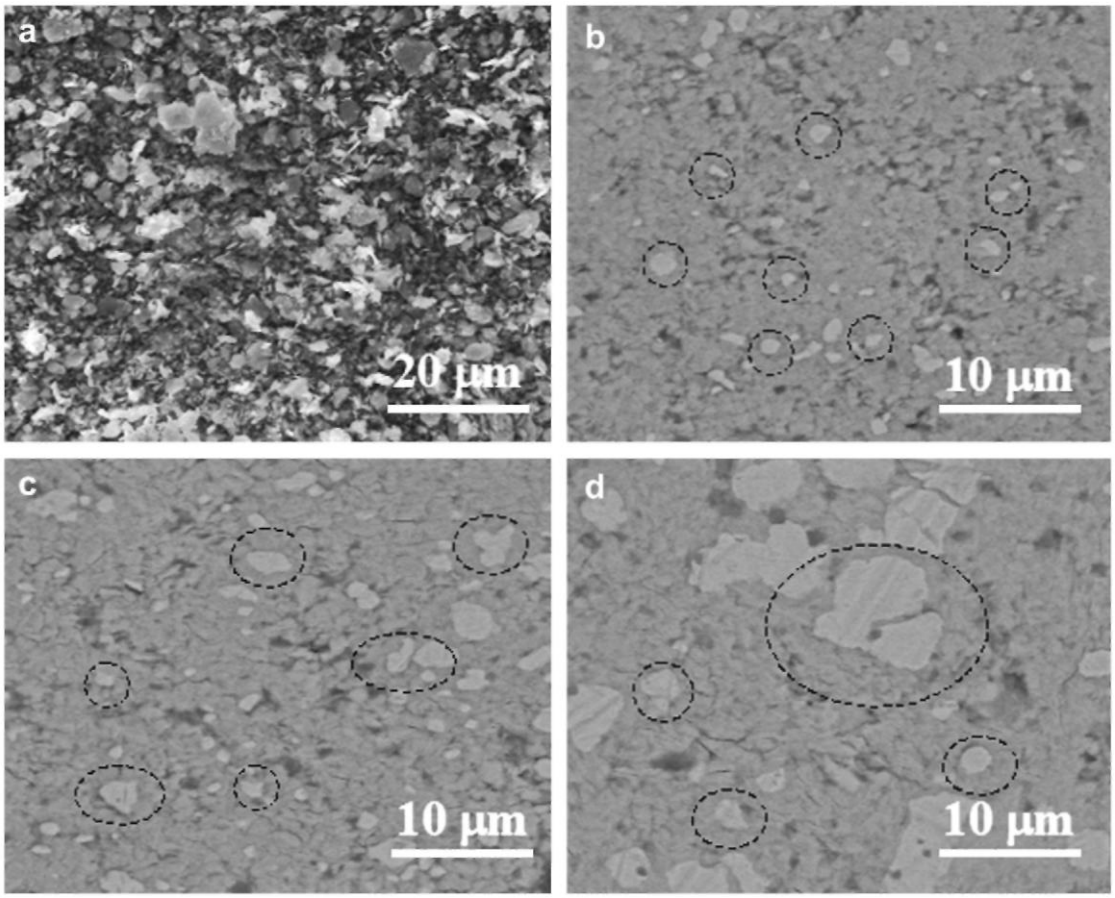

Density measurements (Table 1) show that the density of the uniaxial pellets decreases when the Ag content increases up to 20 wt%, because the spherical Ag particles disrupt the stacking of the BCCO platelets. At Ag 30 wt%, the large agglomerates cause an increase of the relative density. For isostatic packing, the sample density is only slightly influenced by the modification of the ratio of anisotropic (BCCO platelets) and isotropic particles (Ag). These relative densities of the samples studied are low, but they are comparable to these obtained by conventional method for other misfit compounds [19].

Fig. 3. *SEM images of a cross-section of (a) uniaxial (parallel to the pressure direction) and (b) isostatic spray-drying samples.*

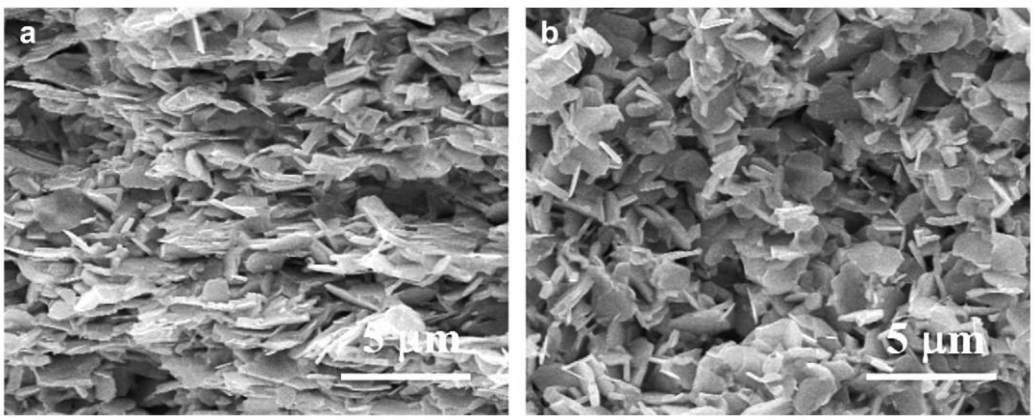

Published in : Solid State Sciences (2010), vol. 12, pp. 1490-1495.
Status : Postprint (Author's version)

3.2. Thermoelectric characteristics

In this section, we study the influence of the Ag content and pressing method on the electrical conductivity and Seebeck coefficient, which determine the thermoelectric power factor ($P = S^2\sigma$). We will compare the properties of the Ag-BCCO composites prepared by spray-drying with the BCCO sample synthesized by the classical solid state method.

Fig. 4 displays the temperature dependence of the electrical conductivity (σ) from 300 to 1100 K. For all samples, a metallic-like behavior is observed. For the samples without silver, the spray-drying isostatic and the solid state uniaxial BCCO have electrical conductivity values of 20-25 S cm^{-1} at 300 K, in agreement with the value reported by Maignan et al. [23]. The electrical conductivity of the spray-drying uniaxial sample is more than twice higher (56 S cm^{-1} at 300 K). This last result confirms the interest of spray-drying technique which leads to an improvement of the electrical conductivity similar to the one obtained by hot forging technique [28]. This feature is a consequence of the more homogeneous particle size distribution which allows a better c-axis grain stacking, a better connectivity between grains and more homogeneous grain boundaries. Similar results were reported by other authors for $[(Bi,Pb)_2Ba_2O_4]^{RS}[CoO_2]_2$ cobaltite prepared by spray-drying technique [40].

In the case of the Ag-BCCO composites prepared by spray-drying, the electrical conductivity of the isostatically-pressed samples is always lower than that of the uniaxial samples. Indeed, the random distribution of the particles means that conductivity occurs not only in the low-resistivity ab planes of the CoO_2 layers but also through the high-resistivity rock-salt blocks (along the c direction) [18]. In the composite samples, the electrical conductivity systematically increases with the Ag content, except for the uniaxial sample with 30 wt% Ag. In the uniaxial Ag-BCCO composites with low Ag content (10 or 20 wt%), the small Ag particles promote the electrical connections at the grain boundaries of the BCCO particles, reducing the carrier scattering. This effect is more important and compensates for the decrease of density. For the uniaxial sample with 30 wt% Ag, the decrease of electrical conductivity is probably due to the presence of larger silver agglomerates (see Fig. 2d). They possibly disturb the alignment of the BCCO particles and the electrical conductivity, indeed this sample shows similar values to the isostatic sample. For isostatic samples, increasing the Ag content increases the electrical conductivity (maximum value of 41 S cm^{-1} at 300 K). Due to the random distribution of the BCCO particles in these samples, the conductivity is mainly improved by the better electrical connections through the Ag particles.

Fig. 4. *Electrical conductivity as a function of temperature for BCCO sample and Ag-BCCO composites. Close and open symbols are for the uniaxial (Uni) and isostatic (Iso) samples, respectively.*

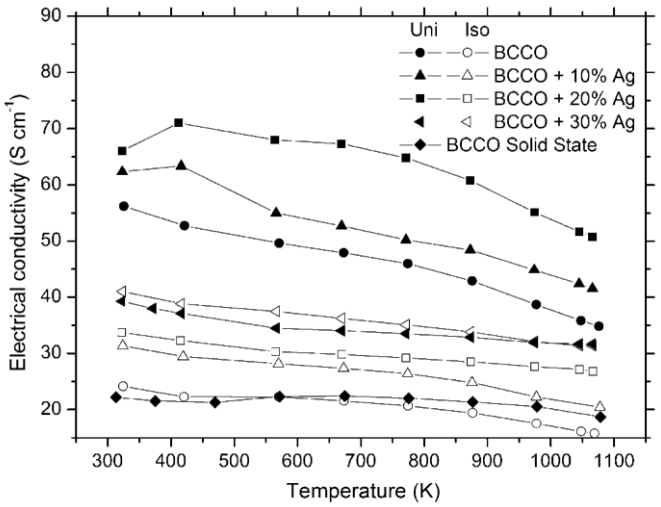

Fig. 5. *Seebeck coefficient as a function of temperature for BCCO sample and Ag-BCCO composites. Close and open symbols are for the uniaxial (Uni) and isostatic (Iso) samples, respectively.*

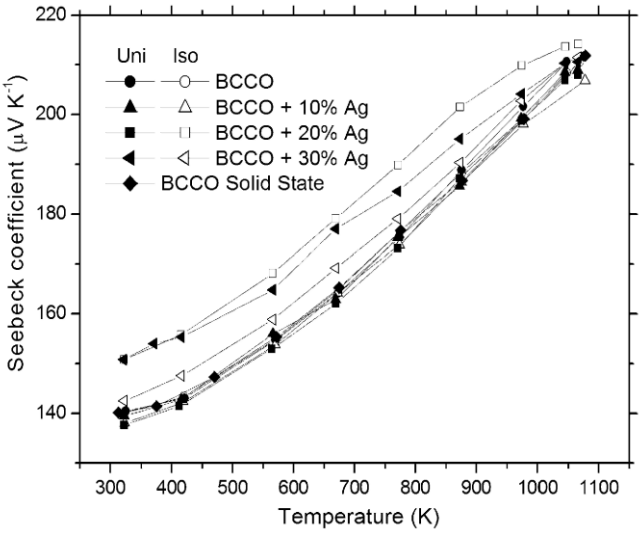

Fig. 5 shows the Seebeck coefficient as a function of temperature. For all samples, positive values are observed and indicate a hole carrier conduction, typical of the layered cobaltites [18,23,28]. The minimum value is 140 μV K^{-1} at 325 K and increases almost linearly up to a maximum of 210 μV K^{-1} at ~1075 K. These values are in agreement with those reported in the literature for single BCCO phase [18,23]. The Seebeck coefficient is not significantly affected by the Ag addition, except for the isostatic sample with 20 wt% Ag and the uniaxial sample with 30 wt% Ag, where a small increase is observed (less than 10 μV K^{-1}). In the literature, the Seebeck coefficient of $Ca_3Co_4O_9$ usually decreases in the case of Ag-CCO composites and increases in the case of Ag substitution [26,27,30,31,41]. The data for $Na_xCoO_{2-\delta}$ are less clear and it is difficult to define a trend [24,32], mainly due to the presence of secondary phases. In the present case for Ag-BCCO, the Seebeck coefficient is unchanged or slightly increased, which confirms that the spray-drying method results in a well separated Ag particles in the BCCO matrix, avoiding the reduction of the Seebeck coefficient by a bypass effect [26].

The electrical conductivity and the Seebeck coefficient are combined in the power factor to evaluate the thermoelectric performance of the samples. The temperature dependence of the power factor is shown in Fig. 6. For all samples, the power factor increases monotonically with temperature and mainly reveals the evolution of the electrical conductivity. The values obtained for the spray-drying isostatically-pressed samples are always lower than for the uniaxially-pressed samples. However, the value for the spray-drying isostatic BCCO sample is comparable to that of solid state BCCO sample. The best results are obtained for the spray-drying uniaxial sample with 20 wt% Ag, with an interesting value almost 3 times higher than the value attained by the solid state BCCO, reaching a maximum value of 2.2 μW K^{-2} cm^{-1} at ~1050 K. This value is smaller than those achieved by intermetallic materials (see Introduction) but comparable with those obtained by the classic solid state method for $Ca_3Co_4O_9$ and $Ca_{2.25}Bi_{0.75}Co_4O_9$ (1.16 μW K^{-2} cm^{-1} and 1.9 μW K^{-2} cm^{-1} at ~1000 K, respectively [20]).

Fig. 6. *Power factor as a function of temperature for BCCO sample and Ag-BCCO composites. Close and open symbols are for the uniaxial (Uni) and isostatic (Iso) samples, respectively.*

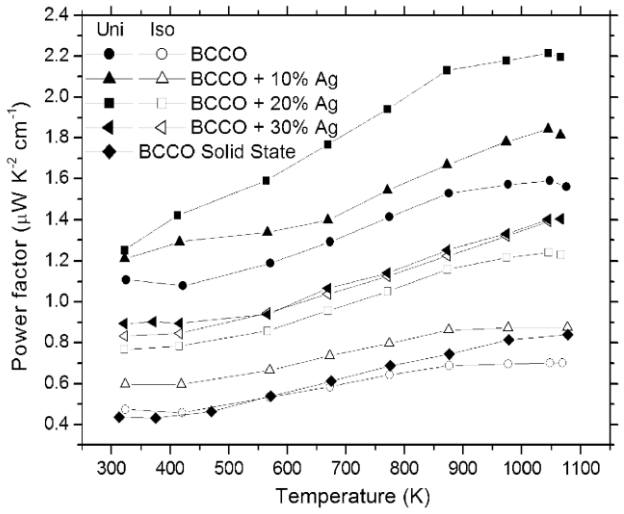

4. Conclusion

$[Bi_{1.68}Ca_2O_4]^{RS}[CoO_2]_{1.69}$ (BCCO) sample and Ag-BCCO composites (Ag 10, 20 and 30 wt%) were synthesized by the spray-drying technique. The presence of the metallic Ag phase at the grain boundaries leads to an increase of the electrical conductivity, while the Seebeck coefficient is not very much affected. Uniaxial pressing promotes a favorable orientation of the BCCO platelets and the presence of isotropic Ag particles results in a small decrease of the density of the uniaxially-pressed samples at low Ag contents (inferior to 20 wt%). The best results were obtained for the spray-drying uniaxial 20 wt% Ag composite. The power factor is 2.2 $\mu W\ K^{-2}\ cm^{-1}$ at 1050 K, which is 3 times higher than for solid state BCCO. Spray-drying synthesis appears as a promising technique to obtain efficient thermoelectric composites. In fact, this technique presents several important advantages. Firstly, it can be used at industrial scale. Secondly, the silver phase is better dispersed in the matrix than by other solution methods and the large agglomerates appear at higher Ag contents than by the classical solid state mixing method. Consequently, the extension of this method to other composites with Ag or cheaper secondary phases should certainly arouse great interest to improve the efficiency of the thermoelectric materials.

Acknowledgments

Part of this work was supported by the Belgian Science Policy under the Technology Attraction Pole Program (CHEMAT TAP2/03). H. Muguerra would like to thank the University of Liège for his postdoctoral fellowship.

References

[1] G. Mahan, B. Sales, J. Sharp, Phys. Today 50 (1997) 42-47.

[2] R. Ionescu, J. Jaklovszky, N. Nistor, A. Chiculita, Phys. Status Solidi A 27 (1975) 27-34.

[3] D.B. Hyun, J.S. Hwang, B.C. You, Mater. Sci. 33 (1998) 5595-5600.

[4] B.C. Sales, Mater. Res. Soc. Bull. 23 (1998) 15-21.

[5] G.J. Snyder, M. Christensen, E.J. Nishibori, T. Caillat, B.B. Iversen, Nat. Mater. 3 (2004) 458-463.

[6] M.S. Dresselhaus, G. Chen, M.Y. Tang, R. Yang, H. Lee, D. Wang, Z. Ren, J.-P. Fleurial, P. Gogna, Adv. Mater. 19 (2007) 1043-1053.

[7] M.G. Kanatzidis, Chem. Mater. 22 (2010) 648-659.

[8] T. Nilges, O. Osters, M. Bawohl, J.-L Bobet, B. Chevalier, R. Decourt, R. Weihrich, Chem. Mater. 22 (2010) 2946-2954.

[9] J.-S. Rhyee, K.H. Lee, S.M. Lee, E. Cho, S. I. Kim, E. Lee, Y.S. Kwon, J.H. Shim, G. Kotliar, Nature 459 (2009) 965-968.

[10] I. Terasaki, Y. Sasago, K. Uchinokura, Phys. Rev. B. 56 (1997) R12685-R12687.

[11] S. Li, R. Funahashi, I. Matsubara, K. Ueno, H. Yamada, J. Mater. Chem. 9 (1999) 1659-1660.

[12] Y. Miyazaki, K. Kudo, M. Akoshima, Y. Ono, Y. Koike, T. Kajitani, Jpn. J. Appl. Phys. 39 (2000) L531-L533.

[13] A.C. Masset, C. Michel, A. Maignan, M. Hervieu, O. Toulemonde, F. Studer, B. Raveau, Phys. Rev. B. 62 (2000) 166-175.

[14] R. Funahashi, I. Matsubara, S. Sodeoka, Appl. Phys. Lett. 76 (2000) 2385-2387.

[15] Y. Masuda, D. Nagahama, H. Itahara, T. Tani, W.S. Seo, K. Koumoto, J. Mater. Chem. 13 (2003) 1094-1099.

[16] H. Itahara, C. Xia, J. Sugiyama, J. Mater. Chem. 14 (2004) 61-66.

[17] Y. Zhou, I. Matsubara, S. Horii, T. Takeuchi, R. Funahashi, M. Shikano, J. Shimoyama, K. Kishio, W. Shin, N. Izu, N. Murayama, J. Appl. Phys. 93 (2003) 2653-2658.

[18] E. Guilmeau, M. Mikami, R. Funahashi, J. Mater. Res. 20 (2005) 1002-1008.

[19] I. Matsubara, R. Funahashi, T. Takeuchi, S. Sodeoka, J. Appl. Phys. 90 (2001) 462-465.

[20] S. Li, R. Funahashi, I. Matsubara, K. Ueno, S. Sodeoka, H. Yamada, Chem. Mater. 12 (2000) 2424-2427.

[21] G. Xu, R. Funahashi, M. Shikano, I. Matsubara, Y. Zhou, Appl. Phys. Lett. 80 (2002) 3760-3762.

[22] M. Mikami, R. Funahashi, J. Solid State Chem. 178 (2005) 1670-1674.

[23] A. Maignan, S. Hébert, M. Hervieu, C. Michel, D. Pelloquin, D. Khomskii, J. Phys. Condens. Matter 15 (2003) 2711-2723.

[24] M. Ito, D. Furumoto, Scripta Mater. 55 (2006) 533-536.

[25] M. Ito, D. Furumoto, J. Alloys Compd. 450 (2008) 517-520.

[26] M. Mikami, N. Ando, R. Funahashi, Solid State Chem. 178 (2005) 2186-2190.

[27] Y. Wang, Y. Sui, J. Cheng, X. Wang, W. Su, J. Alloys Compd. 477 (2009) 817-821.

[28] E. Guilmeau, M. Pollet, D. Grebille, D. Chateigner, B. Vertruyen, R. Cloots, R. Funahashi, B. Ouladiaff, Mater. Res. Bull. 43 (2008) 394-400.

[29] Y. Wang, Y. Sui, J. Cheng, X. Wang, J. Miao, Z. Liu, Z. Qian, W. Su, J. Alloys Compd. 448 (2008) 1-5.

[30] Y. Song, Q, Suna, L Zhao, F. Wang, Z. Jiang, Mater. Chem. Phys. 113 (2009) 645-649.

[31] P.-H. Xiang, Y. Kinemuchi, H. Kaga, K. Watari, J. Alloys Compd. 454 (2008) 364-369.

[32] T. Seetawan, V. Amornkitbamrung, T. Burinprakhon, S. Maensiri, K. Kurosaki, H. Muta, M. Uno, S. Yamanaka, J. Alloys Compd. 407 (2006) 314-317.

[33] S.R. Percy, US Patent 125 406, (1872).

[34] F.P. Zhang, Q.M. Lu, J.X. Zhang, X. Zhang, J. Alloys Compd. 477 (2009) 543-546.

[35] V. Petricek, M. Dusek, L. Palatinus, JANA2000: Crystallographic Computing System. Institute of Physics, Prague, 2000.

[36] CAS number 7440-22-4.

[37] H. Muguerra, D. Grebille, E. Guilmeau, R. Cloots, Inorg. Chem. 47 (2008) 2464-2471.

[38] R.D. Shannon, Acta Cryst. A 32 (1976) 751-767.

[39] H. Yakabe, K. Fujita, K. Nakamura, K. Kikuchi, Proceedings of the 17th International Conference on Thermoelectrics (1998) 551-558.

[40] T. Motohashi, Y. Nonaka, K. Sakai, J. Appl. Phys. 103 (2008) 033705 6 pp.

[41] Y. Wang, Y. Sui, J. Cheng, X. Wang, W. Su, J. Phys. Condens. Matter 19 (2007) 356216 10 pp.